DØCONF note 5200

Measurement of the Top Quark Mass in the $e\mu$ Channel Using the Matrix Weighting Method at DØ

The DØ Collaboration
URL http://www-d0.fnal.gov
(Dated: July 24, 2006)

We present a preliminary measurement of the top quark mass in the $e\mu$ channel based on about 835 pb^{-1} of data collected by the DØ experiment during Run II of the Fermilab Tevatron collider. We show that the method used obtains consistent results using ensemble tests of events generated with the DØ Monte Carlo simulation. We apply our technique to the $e\mu$ events from the collider data to obtain $m_t = 177.7 \pm 8.8(stat)^{+3.7}_{-4.5}(syst)$ GeV.

Preliminary Results for ICHEP Conference

I. INTRODUCTION

We present a measurement of the top quark mass based on about 835 pb^{-1} of data from $p\bar{p}$-collisions at $\sqrt{s}$=1.96 TeV collected by the DØ experiment during Run II. The method used is similar to that used by the DØ Collaboration to measure the top quark mass in the $e\mu$ channel using Run I data [1].

The top quark mass is an important parameter in standard model predictions. Loops involving top quarks provide the dominant radiative corrections to the value of the W boson mass, for example. Another important correction to the W boson mass originates from loops involving the Higgs boson. Thus precise measurements of the W boson and top quark masses provide a constraint on the Higgs boson mass.

The measurement in the $e\mu$ channel is statistically limited and of less precision than the measurement in the lepton+jets channel. However it provides a complementary measurement of the top quark mass and a consistency check on the $t\bar{t}$ hypothesis in the $e\mu$ channel. With increasing data samples, the mass measurement in this channel will become competitive with that in the lepton+jets channel.

II. THE DØ DETECTOR

The DØ detector is a typical multipurpose collider detector, that consists of central tracking, calorimeter, and muon detection systems.

The magnetic central-tracking system is comprised of a silicon microstrip tracker and a scintillating fiber tracker, both located within a 2 T superconducting solenoidal magnet [2]. Central and forward preshower detectors are located just outside of the coil and in front of the calorimeters. The liquid-argon/uranium calorimeter is divided into a central section covering pseudorapidity $|\eta| \leq 1$ and two end calorimeters extending coverage to $|\eta| \leq 4$ [3]. In addition to the preshower detectors, scintillators between the calorimeter cryostats provide sampling of developing showers at $1.1 < |\eta| < 1.4$. The muon system is located outside the calorimeter and consists of a layer of tracking detectors and scintillation trigger counters before 1.8 T toroids, followed by two similar layers outside the toroids. Tracking at $|\eta| < 1$ relies on 10 cm wide drift tubes [3], while 1 cm mini-drift tubes are used at $1 < |\eta| < 2$.

The trigger and data acquisition systems are designed to accommodate the high luminosities of Run II. Based on information from tracking, calorimeter, and muon systems, the output of the first level of the trigger is used to limit the rate for accepted events to ≈1.5 kHz. At the next trigger stage, with more refined information, the rate is reduced further to ≈800 Hz. These first two levels of triggering rely mainly on hardware and firmware. The third and final level of the trigger, with access to all of the event information, uses software algorithms and a computing farm, and reduces the output rate to ≈50 Hz, which is written to tape.

III. EVENT SELECTION

The event selection closely follows the selection developed previously for the $e\mu$ analysis. The basic idea is to select a single isolated high p_T electron, to pair that with an isolated high p_T muon with opposite charge, and to then demand 2 or more high p_T jets The exact cuts are listed below.

Events must satisfy

- electron:
  - cut on the transverse momentum and pseudorapidity: $p_T(e) > 15$ GeV and $|\eta| < 1.1$ or $1.5 < |\eta| < 2.5$
  - high energy fraction in EM part of the calorimeter $f_{EM} = \frac{E_{EM}}{E_{tot}} > 0.9$
  - isolated EM cluster: $f_{iso} = \frac{E_{tot}(R<0.4) - E_{EM}(R<0.2)}{E_{tot}(R<0.2)} < 0.15$
  - cut on the Electron Likleihood Discriminant > 0.85;
  - require a match between the EM cluster and a track with $p_T > 5$ GeV
  - no common track with a muon
  - veto second electron
- muon:
  - $p_T(\mu) > 15$ GeV and $|\eta| < 2$
  - medium quality

- timing cuts against cosmics
- matched with central track
- cut on distance of closest approach (DCA) in transverse plane : $|DCA| < 0.02$ cm for tracks with SMT hits, $|DCA| < 0.2$ cm for tracks without SMT hits
- track and calorimeter isolation cuts.

- electron must be matched with opposite charge muon with highest p_T.
- require 2 or more jets with $p_T(j) > 20$ GeV and $|\eta| < 2.5$;
- require $H_T^l = \max(p_T(e), p_T(\mu)) + p_T(j_1) + p_T(j_2) > 120$ GeV.

TABLE I: Expected and observed $e\mu$ event yield from background and signal processes.

$t\bar{t}$	WW	$Z \to \tau\tau$	fake e	total background	total	observed
20.2 ± 2.7	$1.24^{+2.2}_{-0.5}$	$2.7^{+1.5}_{-1.3}$	0.4 ± 0.2	$4.4^{+2.6}_{-1.4}$	$24.6^{+3.8}_{-3.0}$	28

Table I gives the expected and observed number of events. This selection starts with the $t\bar{t} \to e\mu$ cross section analysis, but requires that the electron likelihood be greater than 0.85 to significantly lower the fake electron background.

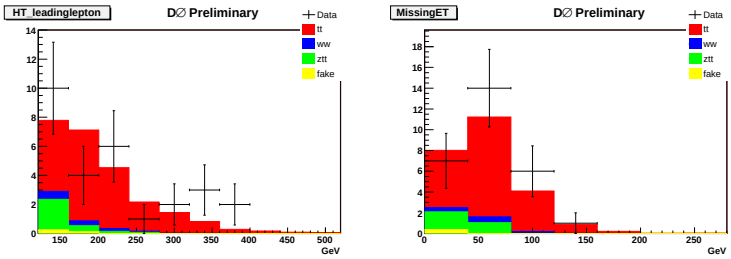

FIG. 1: H_T^l and $\not\!\!E_T$ distributions after all cuts.

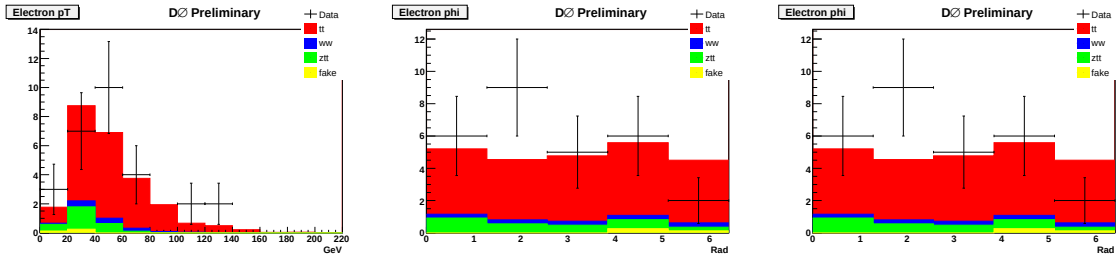

FIG. 2: Electron p_T, η and ϕ distributions after all cuts.

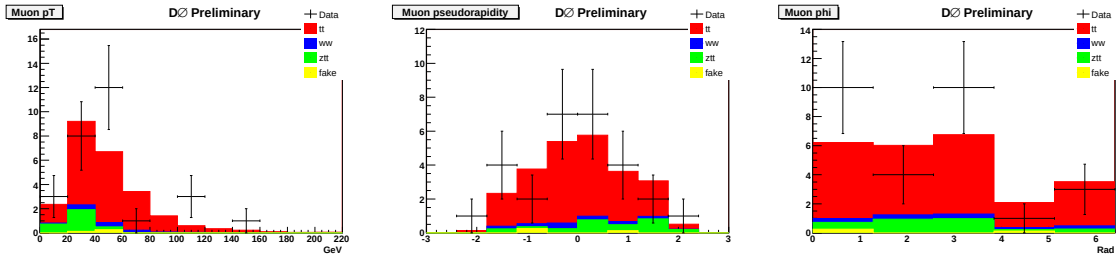

FIG. 3: Muon p_T, η and ϕ distributions after all cuts.

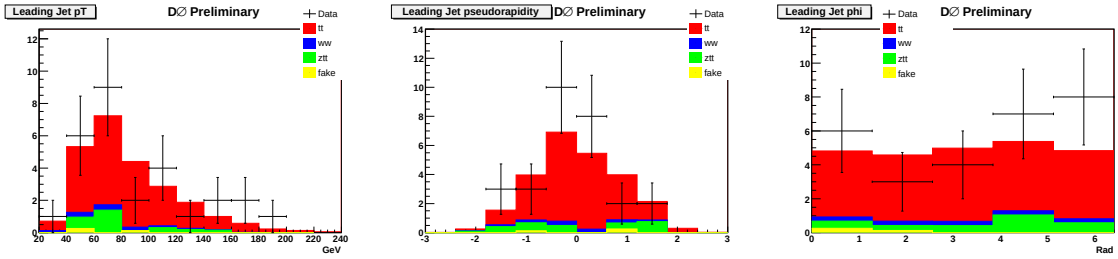

FIG. 4: Leading Jet p_T, η and ϕ distributions after all cuts.

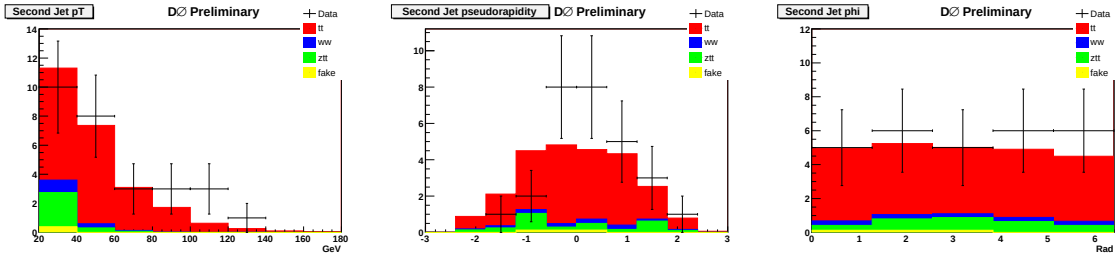

FIG. 5: Second Jet p_T, η and ϕ distributions after all cuts.

IV. ANALYSIS TECHNIQUE

As in the Run I publication [1], we follow the ideas proposed by Dalitz and Goldstein [9] to reconstruct events from decays of top-antitop quark pairs with two charged leptons (either electrons or muons) and two or more jets in the final state. Kondo has published similar ideas [10].

We use only the two jets with the highest p_T in this analysis. We assign these two jets to the b and $\bar{b}$ quarks from the decay of the t and $\bar{t}$ quarks. If we assume a hypothesized value for the top quark mass we can determine the pairs of t and $\bar{t}$ momenta that are consistent with the observed lepton and jet momenta and missing p_T. We call a pair of top-antitop quark momenta that is consistent with the observed event a solution. We assign a weight to each solution, given by

$$w = f(x)f(\overline{x})p(E_\ell^*|m_t)p(E_{\overline{\ell}}^*|m_t),$$

where $f(x)$ is the parton distribution function for the proton for the momentum fraction x carried by the initial quark, and $f(\overline{x})$ is the corresponding value for the initial antiquark. The quantity $p(E_\ell^*|m_t)$ is the probability for the hypothesized top quark mass m_t that the lepton ℓ has the observed energy in the top quark rest frame [9].

There are two ways to assign the two jets to the b and $\bar{b}$ quarks. For each assignment of observed momenta to the final state particles, there may be up to four solutions for each hypothesized value of the top quark mass. The likelihood for each value of the top quark mass m_t is then given by the sum of the weights over all the possible solutions:

$$W_0(m_t) = \sum_{solutions} \sum_{jets} w_{ij}.$$

In the mass analysis procedure described so far we implicitly assume that all momenta are measured perfectly. The weight $W_0(m_t)$ therefore is zero if no exact solution is found. However, the probability to observe this event if the top quark mass has the value m_t does not have to be zero if no exact solution is found, because of the finite resolution of the momentum measurements. We account for this by repeating the weight calculation with input values for the electron, jet, and muon momenta that are drawn from distributions which match the known detector resolutions. For electrons, the momentum is drawn from a gaussian distribution centered at the observed momenta, with a width given by:

$$\frac{\sigma(E)}{E} = C \oplus S/\sqrt{E} \oplus N/E$$

Where C and N are constants, and S is a function of the energy E and pseudorapidity η. For jets the momenta are drawn from a double-gaussian distribution, which has been tuned to reflect the relationship between observed jets

and partons in Monte Carlo [14]. For the muon the inverse momenta are drawn from a gaussian distribution with an η dependent width.

The missing p_T is corrected by the vector sum of the differences in the particle momenta from the measured values and an added random noise vector. We then average the weight curves obtained from N such variations:

$$W(m_t) = \frac{1}{N}\sum_{n=1}^{N} W_n(m_t).$$

We thus effectively integrate the weight $W(m_t)$ over the final state parton momenta, weighted by the experimental resolutions. We refer to this procedure as resolution sampling. The main rationale for employing resolution sampling is that it increases the number of events for which we find solutions. In Monte Carlo events with an input top quark mass of 175 GeV, about 10% of the events have no solutions as measured. After sampling 500 times for each event the fraction of events without solutions drops to less than 1%.

For each event we use the value of the hypothesized top quark mass at which $W(m_t)$ reaches its maximum as the estimator for the mass of the top quark. We call this mass value the peak mass. We cannot determine the top quark mass directly from the distribution of peak masses, because effects such as initial and final state radiation shift the most probable value of the peak mass distribution away from the actual top quark mass. We therefore generate the expected distributions of weight curve peaks for a range of top quark masses using Monte Carlo simulations. We call these distributions templates.

All Monte Carlo samples used in this analysis were generated using PYTHIA [12] as the event generator, and GEANT [13] for the detector simulation. Weights have been applied to events to account for electron and muon identification efficiencies, the Z p_T spectra in Monte Carlo, and the efficiency to pass DØ trigger system requirements. Jets in monte carlo have also been modified using the smearing and removal prescription of the Jet Smearing Shifting and Removal (JSSR) procedure [6].

In calculating event efficiencies the following set of monte carlo samples were considered:

- inclusive $t\bar{t}$ at $m_t = 175$ GeV for the signal.
- $WW \to ll$ and incusive $Z \to \tau\tau$ for the physics backgrounds.
- The number of fake electron events was estimated using a fit to the electron likelihood [5], while the distribution of peak masses was extracted using same sign $e\mu$ events in the data.

Additional samples were included for the mass analysis:

- $t\bar{t} \to inclusive$ with 13 different top masses in the range $140 - 230$ GeV
- $t\bar{t} \to ll$ with 9 different top masses in the range $155 - 195$ GeV (used to increase statistics)
- $Z \to \tau\tau \to e\mu$ where both electron and muon are required to have $p_T > 10$ GeV before the detector simulation is run.

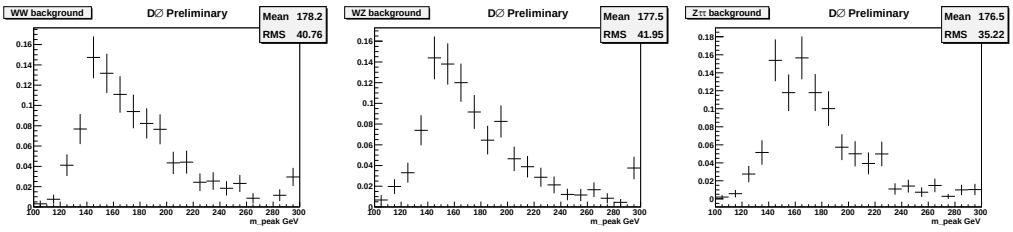

FIG. 6: Peak mass spectra for WW, $Z \to \tau\tau$, and fake electron background in the $e\mu$ channel.

V. ANALYSIS OF EVENTS FROM DØ COLLIDER DATA

We use the Monte Carlo templates with the nominal background contribution levels to fit the events from collider data. The likelihood is maximized for $m_t = 177.9 \pm 8.7$ GeV.

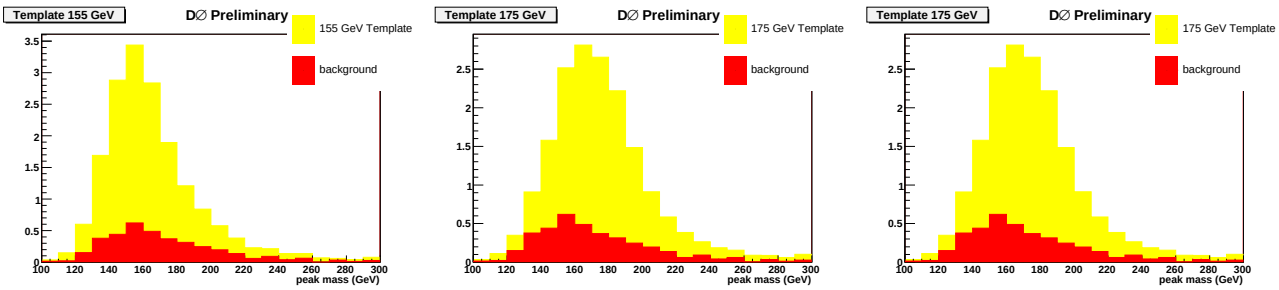

FIG. 7: Templates from Monte Carlo events from $t\bar{t}$ decays to $e\mu$ for m_t=155 GeV (left), 175 GeV (center), and 195 GeV (right). The red histogram represents the expected background contribution.

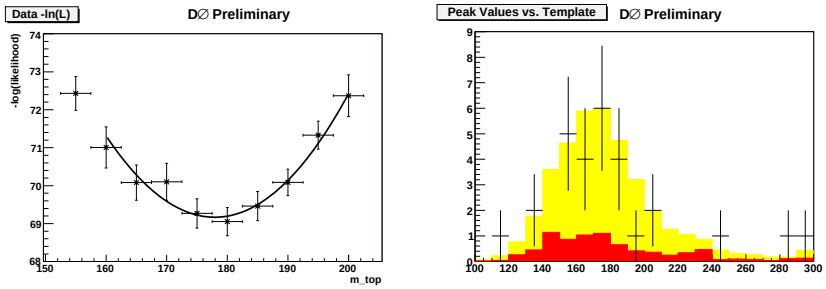

FIG. 8: Plots of $-\ln L$ versus top quark mass (left) and comparison of peak masses in data and Monte Carlo (right).

VI. PERFORMANCE WITH DØ MONTE CARLO EVENTS

In order to demonstrate the performance of our method, we generate a large number of simulated experiments for several input top quark mass values. We refer to each of these experiments as an ensemble. We fit each of the ensembles to the templates as for collider data. The distribution of measured top quark mass values from the ensemble fits gives an estimate of the parent distribution of our measurement.

For ensemble tests events are taken from the signal and background samples with probabilities that correspond to the fraction of events expected from each sample. We calculate $-\ln L$ at each mass point using the templates for the $e\mu$ final state, then we add $-\ln L$ and fit the joint likelihood versus top quark mass in the same way as for the collider data.

Table II lists the result of the ensemble tests, and Figure 9 shows the plot of average fitted mass versus input top quark mass. We fit straight lines to these points. The slope of the lines are consistent with 1.0. The small offsets lead to corrections to the final results. The pull rms values average to 1.04 ($pull = (m_{fit} - m_{true})/\sigma_m$), indicating that the error determined from the point at which $-\ln L$ changes by half a unit slightly underestimates the statistical uncertainty. We therefore correct the statistical errors obtained from the fit by multiplying them with the respective average pull width.

TABLE II: Results of ensemble tests for events drawn randomly from signal and background templates.

m_t	$\langle m_{fit} \rangle$	RMS(m_{fit})	$\langle$pull$\rangle$	RMS(pull)
155 GeV	156.914 GeV	9.07002 GeV	0.185845	0.991481
160 GeV	161.538 GeV	9.32501 GeV	0.178183	0.979587
165 GeV	164.912 GeV	8.75117 GeV	-0.0361073	0.974849
170 GeV	171.421 GeV	9.06555 GeV	0.127242	0.959628
175 GeV	175.619 GeV	10.1769 GeV	0.0616974	1.02648
180 GeV	180.912 GeV	10.0892 GeV	0.0672742	1.05034
185 GeV	184.601 GeV	10.3049 GeV	-0.0789792	1.05147
190 GeV	189.218 GeV	10.7092 GeV	-0.0944111	1.09849
195 GeV	194.043 GeV	10.4185 GeV	-0.133999	1.07829

We use the ensemble test technique to study the size of the systematic uncertainties. We make systematic changes

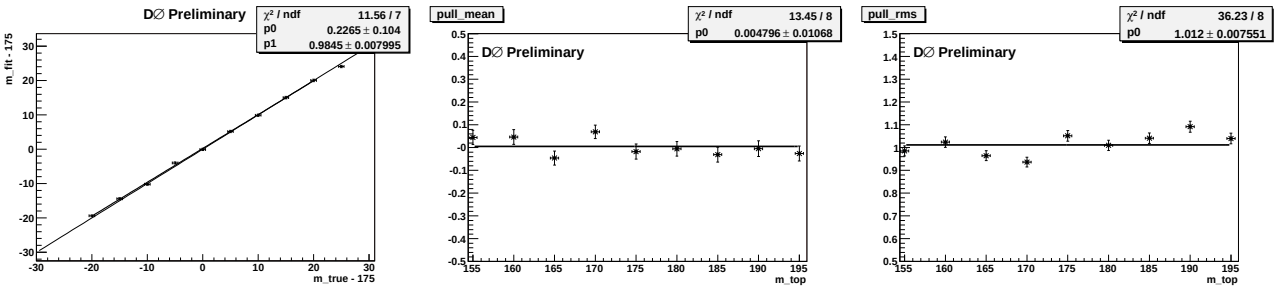

FIG. 9: Average fit mass, pull, and pull width versus input top quark mass for the ensemble tests.

to the events in the ensembles and fit them using the nominal templates. The change in the result gives the size of the systematic uncertainty.

Since we compare the results from the collider data against simulated templates, the measurement will be systematically biased if the jet energies are calibrated differently in data and simulation. The jet energy scale uncertainties are parameterized in terms of the uncorrected p_T and η of the jet, and to estimate the effect of these uncertainties , we generate two sets of ensembles, one with the p_T values of all jets decreased by one sigma (where sigma is different for each jet) and the other with the jet p_T increased by one sigma, and fit both with the nominal templates. The results are shown in Fig. 10. At $m_{top} = 177$ GeV, the average fitted mass increases by 3.5 GeV for the sample shifted down, and decreases by 3.9 GeV for the sample shifted up.

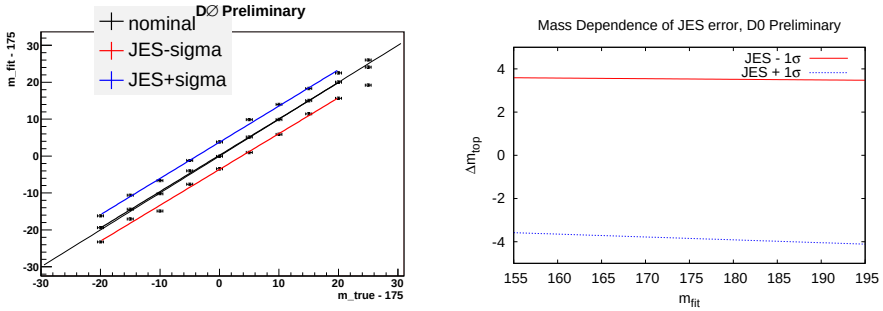

FIG. 10: Average fit mass versus input top quark mass for ensemble tests with the jet scale varied by $\pm 1\sigma$ (left). Change in top quark mass for the jet energy scale variations as a function of the fitted mass (right).

In order to estimate the effect of the uncertainty in the background estimation on the result, we increase and decrease the expected signal-to-background ratio from Table I in the ensembles by one sigma while keeping the nominal templates, this is useful as the method is not sensitive to shifts in the overall number of events, only to the relative contribution of signal and background. At $m_{top} = 177$ GeV the fitted mass shifts down by 1.9 GeV for the sample with S/B decreased by 1 sigma, and the fitted mass shift up by 0.3 GeV in the sample with S/B increased by 1 sigma.

We have not at this point evaluated the systematic variations due to parton distribution function uncertainties, gluon radiation, calibration, and template statistics, seperately for the new analysis and instead rely on the systematics obtained in the previous analysis [7].

VII. RESULT

The fit results have to be corrected for the small offsets observed in the calibration (see Figure 9) and for the pull widths. The calibrated result is $m_t = 177.7 \pm 8.8(stat)^{+3.7}_{-4.5}(syst)$ GeV. Table III summarizes the uncertainties. The world average top quark mass measurement based on Run I and Run II data collected by CDF and DØ is $m_t = 172.7 \pm 2.9$ GeV [16]. Our result is perfectly consistent with the world average value.

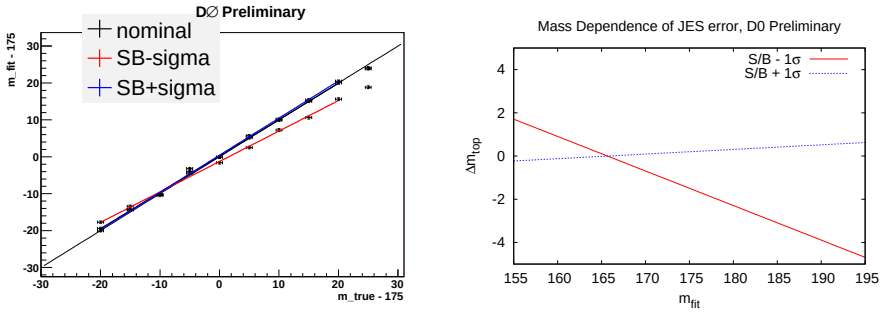

FIG. 11: Average fit mass versus input top quark mass for ensemble tests with the signal fraction varied by $\pm 1\sigma$ (left). Change in top quark mass for the signal fraction variations as a function of the fitted mass (right).

TABLE III: Summary of uncertainties.

source	uncertainty
statistical	8.8 GeV
systematic	+3.7 −4.5 GeV
jet energy scale	+3.5 −3.9 GeV
background	+0.3 −1.9 GeV
parton distribution functions	0.8 GeV
gluon radiation	0.7 GeV
calibration	0.5 GeV
template statistics	0.3 GeV
total	+9.6 −9.9 GeV

VIII. CONCLUSION

In this paper we present a preliminary measurement of the top quark mass in the dilepton channel. We show that the method used gives consistent results using ensemble tests of events generated with the DØ Monte Carlo simulation. We apply our technique to the dilepton events found in the collider data and obtain $m_t = 177.7^{+9.6}_{-9.9}$ GeV.

[1] DØ Collaboration, Phys. Rev. Letters 80, 2063 (1998); Phys. Rev. D 60, 052001 (1999).
[2] DØ Collaboration, V. Abazov *et al.*, "The Upgraded DØ Detector", submitted to Nucl. Instrum. Methods Phys. Res. A, and T. LeCompte and H.T. Diehl, Ann. Rev. Nucl. Part. Sci. **50**, 71 (2000).
[3] DØ Collaboration, S. Abachi *et al.*, Nucl. Instrum. Methods Phys. Res. A **338**, 185 (1994).
[4] DØ note 4850-CONF, "Measurement of the $t\bar{t}$ Production Cross Section at $\sqrt{s} = 1.96$ TeV in Dilepton Final States using 370 pb^{-1} of DØ Data", July 2005.
[5] DØ note 4877, "Measurement of the $t\bar{t}$ Production Cross-section at $\sqrt{s} = 1.96$ TeV in Electron Muon Final States", May 2006.
[6] DØ note 4914, "Shifting, Smearing, and Removing Simulated Jets", November 2005.
[7] DØ note 4997, "Measurement of the Top Quark Mass in the Dilepton Channel",February 2006.
[8] DØ note 4818, "Determination of the Muon Transfer Function for Top Mass Measurements", June 2005.
[9] R.H. Dalitz and G.R. Goldstein, Phys Rev. D 45, 1531 (1992).
[10] K. Kondo, J. Phys. Soc. Jpn. 57, 4126 (1988); 60, 836 (1991).
[11] M.L. Mangano, M. Moretti, F. Piccinini, R. Pittau, A. Polosa, JHEP 0307:001,2003, hep-ph/0206293; M.L. Mangano, M. Moretti, R. Pittau, Nucl.Phys.B632:343-362,2002; hep-ph/0108069; F. Caravaglios, M. L. Mangano, M. Moretti, R. Pittau, Nucl.Phys.B539:215-232,1999; hep-ph/9807570.
[12] T. Sjöstrand et al., Computer Physics Commun. 135 (2001) 238.
[13] S. Agostinelli et al., Nuclear Instruments and Methods in Physics Research A506, 250 (2003).
[14] DØ note 4874-CONF "Top Quark Mass Measurement with the Matrix Element Method in the Lepton+Jets Final State at DØ Run II", July 2005.
[15] S. Frixione, P. Nason, B.R. Webber, JHEP08(2003)007.
[16] The CDF and DØ Collaborations, the Tevatron Electroweak Working Group, "Combination of CDF and DØ Results on the Top-Quark Mass", hep-ex/0507091.